

Simulation Standard

TCAD Driven CAD

A Journal for Process and Device Engineers

QUEST

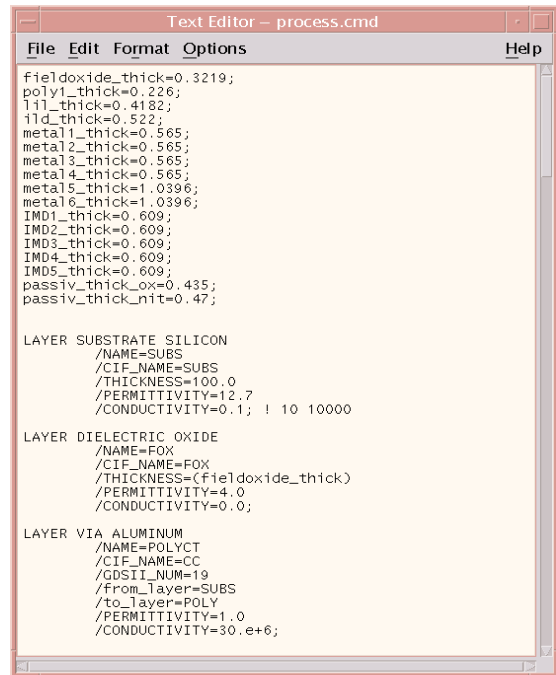
Extraction of Frequency Dependent R, L, C, and G Transmission Line Models

1.0 Introduction

A primary use of *QUEST* is intended to be for extracting frequency dependent transmission line models for use in SPICE circuit simulations.

The generation of SPICE parameters for transmission line models is becoming increasingly important as clock speeds approach and exceed the 1 GHz frequency range. At these speeds many parts of a chip such as data buses, clock lines or power rails can no longer be modeled using simple RC networks. *QUEST* takes this one step further, as not only does it include inductance in the transmission line model but all the parameters in the generated models are frequency dependent.

One example of why this is so important is the physical phenomena called the "skin effect". This effect occurs at high frequencies in the interconnect layers and in the silicon substrate itself. In the interconnect layers at high frequencies the lines self-inductance of the lines may become significant and result in current conduction away from the centre of the interconnect thus changing



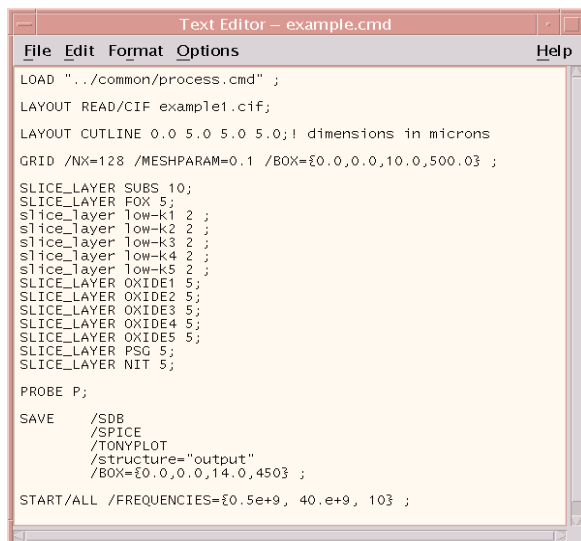
```
fieldoxide_thick=0.3219;
poly1_thick=0.226;
lil1_thick=0.4182;
il1d_thick=0.522;
metal1_thick=0.565;
metal2_thick=0.565;
metal3_thick=0.565;
metal4_thick=0.565;
metal5_thick=1.0396;
metal6_thick=1.0396;
IMD1_thick=0.609;
IMD2_thick=0.609;
IMD3_thick=0.609;
IMD4_thick=0.609;
IMD5_thick=0.609;
passiv_thick_ox=0.435;
passiv_thick_nit=0.47;

LAYER SUBSTRATE SILICON
/NAME=SUBS
/CIF_NAME=SUBS
/THICKNESS=100.0
/PERMITTIVITY=12.7
/CONDUCTIVITY=0.1; ! 10 10000

LAYER DIELECTRIC OXIDE
/NAME=FOX
/CIF_NAME=FOX
/THICKNESS=(fieldoxide_thick)
/PERMITTIVITY=4.0
/CONDUCTIVITY=0.0;

LAYER VIA ALUMINUM
/NAME=POLYCT
/CIF_NAME=CC
/GDSII_NUM=19
/From_layer=SUBS
/to_layer=POLY
/PERMITTIVITY=1.0
/CONDUCTIVITY=30.e+6;
```

Figure 1. Command file of the process that creates the two-dimensional structure.



```
LOAD "../common/process.cmd" ;
LAYOUT READ/CIF example1.cif;
LAYOUT OUTLINE 0.0 5.0 5.0 5.0;! dimensions in microns
GRID /NX=128 /MESHPARAM=0.1 /BOX=£0.0,0.0,10.0,500.03 ;
SLICE_LAYER SUBS 10;
SLICE_LAYER FOX 5;
slice_layer low-k1 2 ;
slice_layer low-k2 2 ;
slice_layer low-k3 2 ;
slice_layer low-k4 2 ;
slice_layer low-k5 2 ;
SLICE_LAYER OXIDE1 5;
SLICE_LAYER OXIDE2 5;
SLICE_LAYER OXIDE3 5;
SLICE_LAYER OXIDE4 5;
SLICE_LAYER OXIDE5 5;
SLICE_LAYER PSG 5;
SLICE_LAYER NIT 5;
PROBE P;
SAVE /SDB
/SPICE
/TONYPLOT
/structure="output"
/BOX=£0.0,0.0,14.0,4503 ;
START/ALL /FREQUENCIES=£0.5e+9, 40.e+9, 103 ;
```

Figure 2. Command file that controls which cutline to operate on and the frequency range under study.

its resistance. The "skin effect" in the silicon substrate can significantly alter the resistance and conductance. These effects will be illustrated by simulations performed by *QUEST* later in this article.

Continued on page 2...

INSIDE

| | |
|---|----|
| Calibrated and Predictive Simulation of Doping Profiles | 4 |
| Using Luminous to Model the Transient Response of a Silicon Charge Collection and Transfer Structure .. | 7 |
| Calendar of Events | 10 |
| Hints, Tips, and Solutions | 11 |

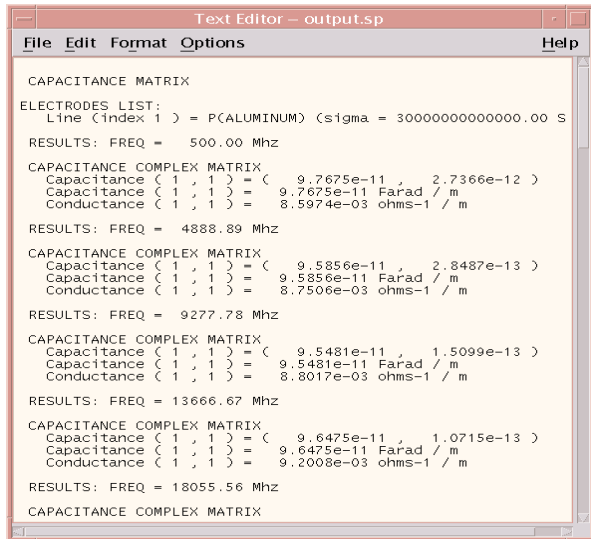


Figure 3. Sample transmission line model that is generated by **QUEST**.

2.0 Major Features of **QUEST**

- (i) The transmission line dimensions are extracted **DIRECTLY** from the chip layout, ie from GDSII or CIF format files using an in-built "Cut-Line" feature.
- (ii) The transmission line structure is built using Process information in combination with the "Cut-Line" feature described above.
- (iii) The cross-section of the conductors can be "trapezoidal" in shape, ie the side-walls do not have to be vertical, thus allowing for more realistic processing effects.
- (iv) The solver uses the "Fictitious Domain" method which has been demonstrated by independent users to be one of the highest speed solving methods around together with being very memory efficient.
- (v) **QUEST** takes full account of the effects of substrate resistivity on the overlying conductors. This can have a significant effect on the RLGC results.

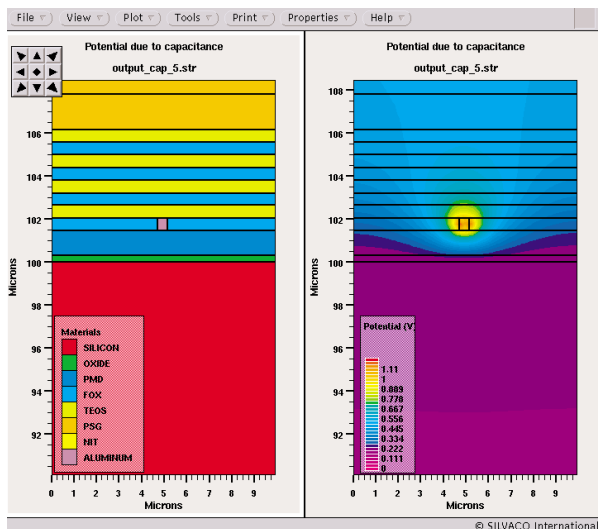


Figure 4. Two-dimensional plot of potential contours.

3.0 Description of Input and Output Formats

The input information for **QUEST** has three basic sets of inputs:

- (i) The mask layout in GDSII, CIF or Silvaco's layout format from which a cutline will be taken defined by the user.
- (ii) Process description file, used in conjunction with the cutline to create the structure for analysis. An example of this syntax is shown in Figure 1.
- (iii) Command file to specify various user defined options as to what to do with the data. An example of this syntax is shown in Figure 2.

There are two basic outputs from **QUEST**:

- transmission line model parameters
- two-dimensional structure files

An example of the extracted transmission line parameters that are output from **QUEST** are shown in Figure 3. All the parameters, R, L, C and G, are frequency dependent. This file can be included into a spice simulation by, for instance, **SmartSpice**.

The internal quantities solved for by **QUEST** may also be saved to a two-dimensional structure file. This file may be viewed by the graphical tool **TonyPlot** for analysis. Figure 4 shows one example of which is a two-dimensional potential contour.

4.0 Effect of High Frequency and Substrate Conductivity on R, L and C.

In this example the transmission line test structure shown in Figure 5 has been used to illustrate how the effect of the substrate changes as the frequency is increased. The structure consists of a single metal line over a substrate. The multi-insulator capability of **QUEST** is required as this structure contains six different insulators.

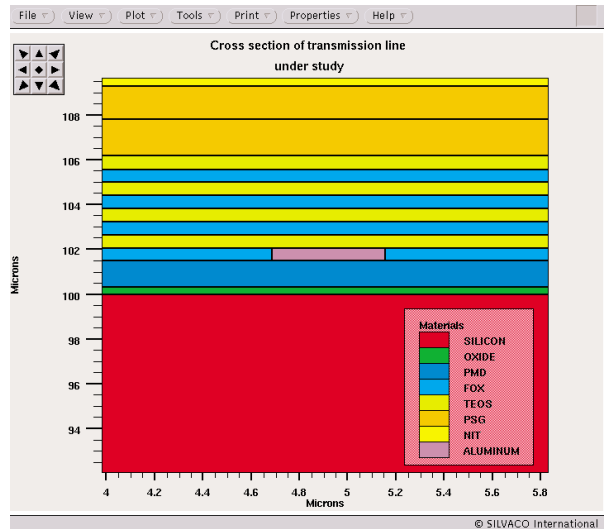


Figure 5. Example test structure of the transmission line to be studied.

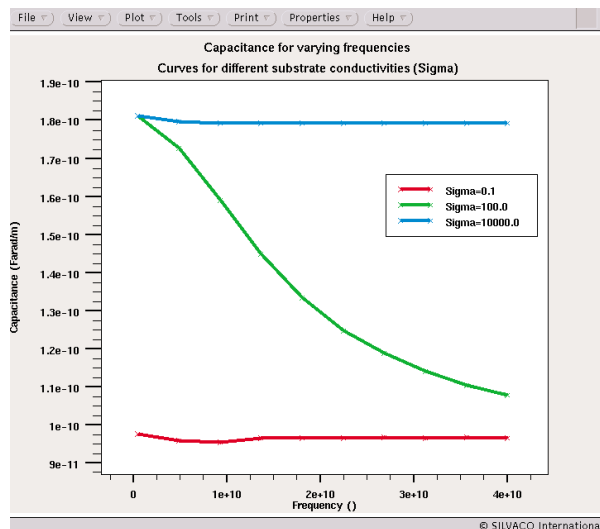


Figure 6. Variation of resistance as the frequency is increased for different substrate conductances.

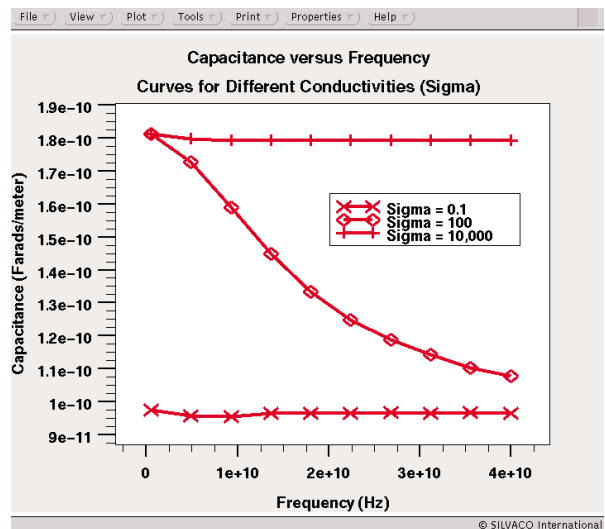


Figure 7. Variation of capacitance with frequency for different substrate conductivity.

The structure is analyzed for the frequency range of 1 to 40 GHz. Figures 6, 7 and 8 illustrate the variation of resistance, capacitance and inductance as a function of frequency. In both experiments the substrate conductivity was varied from a Sigma of 0.1 Siemens/m to 10,000 Siemens/m.

Different behavior is observed in the capacitance and inductance, for different substrate conductivities and for different frequencies (between 1GHz and 40 GHz). For the low conductivity substrate the inductance and the resistance are constant over the frequency range 1-40GHz. However the capacitance C , shows a sharp decrease at high frequencies. For high conductivity substrate two opposite behaviors are observed: the C is constant but the inductance decreases with the frequency.

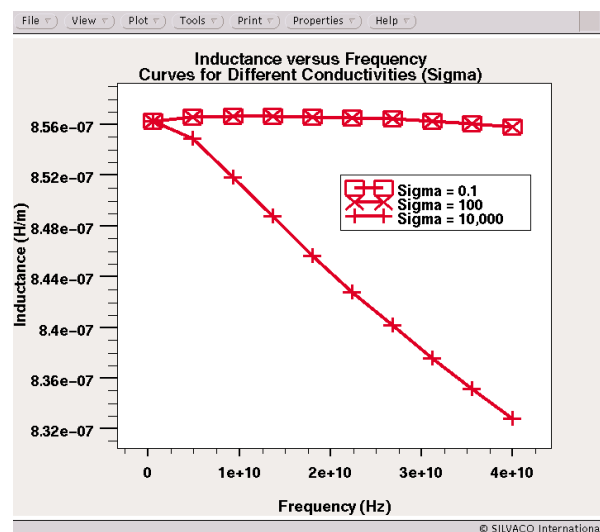


Figure 8. Variation of inductance with frequency for different substrate conductivity.

These phenomena could be explained as the following: at low frequencies and for low substrate conductivities, the substrate behave as a conductor, which results in a large value of the capacitance due to a decrease of the distance between the line and the ground (which is the oxide thickness). At higher frequencies the substrate behave as a dielectric, which results in a decrease of capacitance value due to the increase of the distance between the line and the ground. The resistance and the inductance however, remain nearly constant, since there is no skin effect inside the substrate at low frequencies.

In case of high substrate conductivity, the electrical field is mostly concentrated between the line and the top surface of the substrate, which results in a large value of the capacitance, almost constant over

the frequency range 1-40GHz. However due to the high substrate conductivity there is a significant skin effect inside the substrate. Currents are concentrated on a small region on top of the substrate. Therefore the resistance will increase and the inductance will decrease.

5.0 Conclusions

A unique new product *QUEST* has been introduced which allows a designer to investigate the high frequency behavior of lines within their layout such as clock, power, data lines, etc. With this product a designer may produce a frequency dependent transmission line model which may be used to investigate very accurately the operation of the chip through SPICE simulations. A future article in the Simulation Standard will address the application of models to SPICE design.

Calibrated and Predictive Simulation of Doping Profiles: Low Energy As, B and BF₂ Ion Implantation

P. Scheiblin

LETI (CEA-Grenoble) - 17, rue des Martyrs - 38054 Grenoble Cedex 09 – FRANCE

I. Introduction

This article will present an efficient and original methodology for global and predictive modeling of low energy Boron, BF₂ and Arsenic ion implantation, in the suitable range for sub-100nm CMOS technology.

The International Technology Roadmap for Semiconductors (ed. 1999) underlines the need for development of analytical models for ion implantation simulations, supported by Monte Carlo code. These models become more and more complex, from the simple Gaussian approximations to the latest double Pearson-4 distributions [1], or Legendre polynomials fitting [2].

Leaving apart the domain of the sophisticated ion implantation models, we found that the value of the doping concentration itself could be directly expressed with a fair accuracy, as a function of the experimental conditions. The predictivity of this technique is insured by the use of Design Of Experiments (DoE) and Response Surface Methodology (RSM) [3][4].

This article will explain the methodology used and demonstrate how we can include it in *ATHENA*.

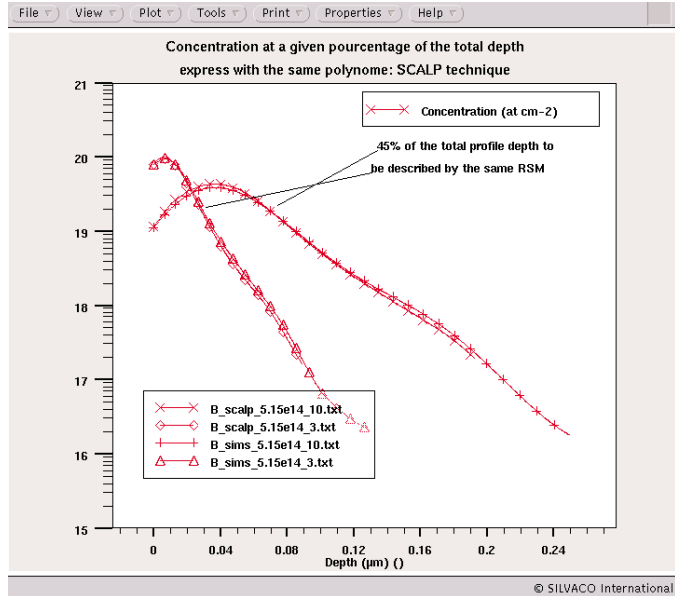


Figure 1: Illustration of the SCALP technique: Each point of the graph (concentration, depth) is calculated using a unique polynomial function, which model the concentration as a function of the total depth (here 45%) whatever the experimental conditions are.

II. New Approach For Modeling Profiles

Usually, the simulation of as-implanted doping profiles is obtained through complex statistical or analytical functions, with parameters depending on the experimental conditions. The tuning of these parameters is not always obvious for achieving a good fit with experiments.

We have decided to express directly the concentration as a function of experimental conditions (dose, energy) with a polynomial. By using DoE to choose the experimental implantation conditions (dose, energy), and RSM for the modeling of the concentrations along the depth, we obtained a predictive and calibrated modeling of the implantation profiles. Figure 1 illustrates the principle of this technique, called Sampling CALibration of Profiles (SCALP): for a given percentage of the total profile depth, one searches a unique polynomial response function for describing the doping concentration, for any combination of the process factors.

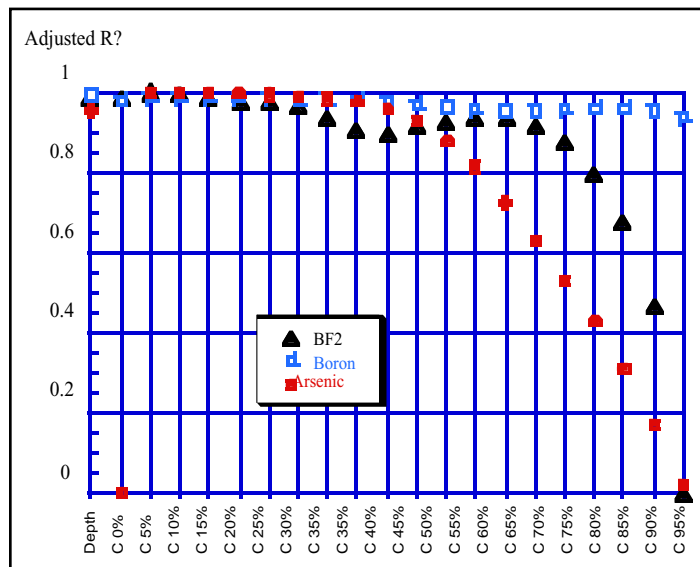


Figure 2: The values of the adjusted R_ higher than 0.8 indicate the quality of the RSM, particularly in the case of B and BF₂

III. Experimental

The experiments were chosen using a 3² design in the aim of obtaining a quadratic modeling of the responses depth and log (concentration), as a function of the factors log(dose) and energy, see Table 1. The center of the design is replicated 3 times on different wafers to estimate the experimental dispersion.

The implantations were performed on 8" wafers, through a 2 nm screen oxide layer, with an EATON NV8200P implanter.

The analysis of these narrow profiles requires carrying out a specific measurement technique [5]: SIMS measurements were performed using a CAMECA IMS-5f with an effective impact energy and incidence angle of 1keV and 60° respectively, in order to reduce ion beam mix-

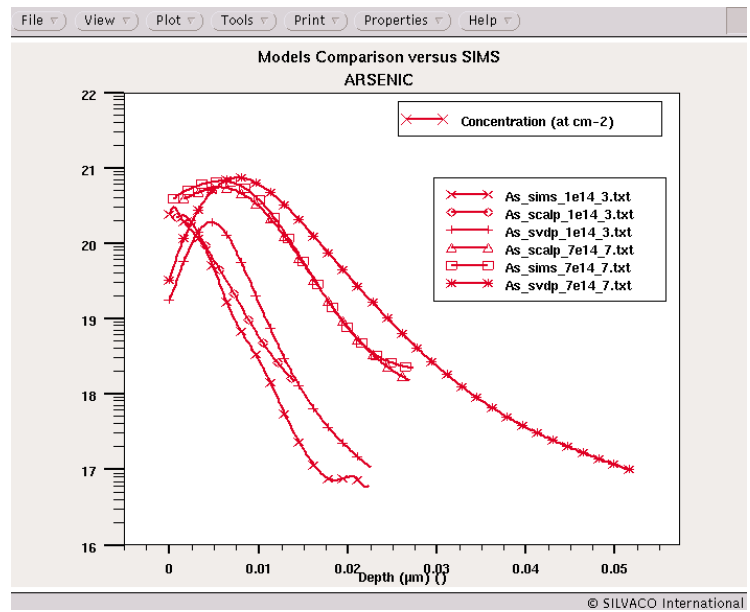


Figure 3: Predictions of Arsenic test points versus SIMS and SVDP.

| Factors | Energy | Dose As BF2 (at. cm ⁻²) | Dose B (at. cm ⁻²) | Tilt (deg) | Twist (deg) |
|---------|---------|--|--|------------|-------------|
| range | 3 to 10 | 3 10 ¹³ to 10 ¹⁵ | 1 10 ¹³ to 5 10 ¹⁴ | 7 | 27 |

Table 1: Experimental ranges for As, BF2 and B.

ing and equilibration depths.

IV. Results and Modelization

The empirical models of the concentrations and depth were generated with the software ECHIP [6]. For all the three dopants, the adjusted R2 were higher than 0.8 until 2/3 of the depth, as shown in Figure 2.

| | Constant | log(d) | W | log(d)*W | log(d)? | W? |
|-------|----------|----------|-----------|-----------|-----------|----------|
| Depth | 1.28E-01 | 3.60E-02 | 1.39E-02 | 3.15E-03 | -8.30E-03 | 2.52E-04 |
| C 0% | 1.86E+01 | 8.53E-01 | -1.14E-01 | -1.13E-02 | 1.47E-01 | 3.25E-02 |
| C 10% | 1.89E+01 | 9.70E-01 | -6.64E-02 | 8.27E-03 | 2.60E-02 | 2.65E-02 |
| C 20% | 1.89E+01 | 8.43E-01 | -2.20E-02 | 2.57E-02 | 3.46E-02 | 2.03E-02 |
| C 30% | 1.88E+01 | 6.87E-01 | 6.69E-03 | 2.67E-02 | 4.64E-02 | 1.60E-02 |
| C 40% | 1.85E+01 | 5.43E-01 | 1.48E-02 | 1.42E-02 | 8.26E-02 | 1.35E-02 |
| C 50% | 1.82E+01 | 4.41E-01 | 1.25E-02 | 5.42E-02 | 1.03E-01 | 1.20E-02 |
| C 75% | 1.76E+01 | 3.27E-01 | 4.96E-03 | 2.06E-03 | 1.05E-01 | 8.71E-03 |

| | Constant | log(d) | W | log(d)*W | log(d)? | W? |
|-------|----------|----------|-----------|-----------|-----------|-----------|
| Depth | 5.97E-02 | 1.99E-02 | 5.57E-03 | 1.07E-03 | -2.46E-03 | -1.01E-04 |
| C 0% | 2.01E+01 | 1.09E+00 | -4.90E-02 | -8.22E-03 | 4.38E-01 | -4.65E-03 |
| C 10% | 2.01E+01 | 8.13E-01 | 1.17E-02 | 3.50E-02 | -1.77E-01 | -1.47E-03 |
| C 20% | 1.94E+01 | 5.27E-01 | 2.86E-02 | 3.78E-02 | -6.34E-03 | 5.34E-03 |
| C 30% | 1.88E+01 | 2.87E-01 | 2.55E-02 | 2.58E-02 | 4.87E-02 | 3.16E-03 |
| C 40% | 1.84E+01 | 1.56E-01 | 2.96E-02 | 2.26E-02 | -2.20E-02 | 3.45E-04 |
| C 50% | 1.82E+01 | 1.00E-01 | 3.44E-02 | 2.13E-02 | -9.18E-02 | -1.03E-03 |
| C 75% | 1.76E+01 | 3.86E-02 | 2.58E-02 | 4.65E-03 | -6.58E-02 | -2.04E-03 |

Table 2: Boron and BF2; centered variables; "d"=dose; "W"=energy.

As an example the coefficients of the quadratic model for Boron and BF2 are given for some concentrations in Table 2. They allow the accurate reconstruction of all the profiles of the DoE, but also any interpolation within the experimental range. Furthermore the simulations are predictive within a 95% confidence interval. Inside this interval, in the case of boron, log(concentration) is predicted at +/-2% and depth at +/-10%. The excellent predictive capability of the models is evidenced in Figure 3 for Arsenic the prediction of the model is superimposed with test points, which have not been used to generate the model.

In Figure 4, we show the global improvement provided by SCALP over the whole As and B profile database, as compared to the simulations performed with the SIMS Verified Dual Pearson (SVDP) model of ATHENA [7]. The improvement is evaluated by the Root Mean Square Relative Error:

$$RMSRE = \sqrt{\sum_{i=1}^n \frac{1}{n} \left(\frac{y_{exp_i} - y_{sim_i}}{y_{exp_i}} \right)^2}$$

where y_{exp_i} and y_{sim_i} are respectively the i^{th} experimental and simulated concentration values of a n points discretization of the profile.

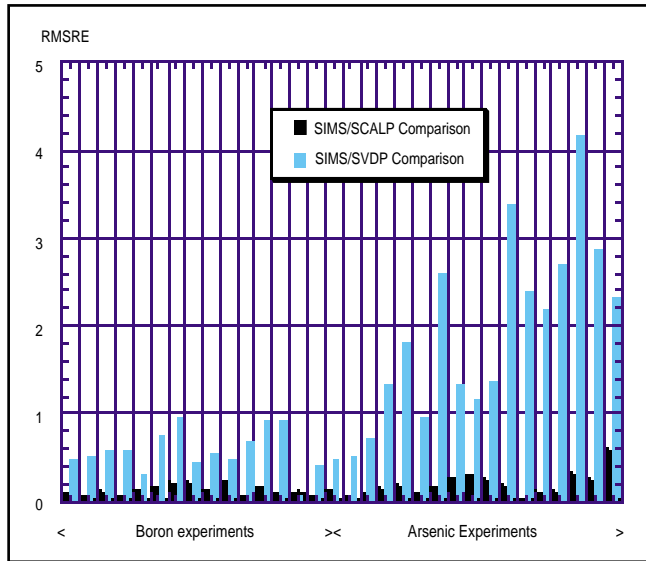


Figure 4. Graph showing the global improvement for As and B.

V. Application to ATHENA

The run-time environment for all SILVACO TCAD simulators, *DeckBuild*, allows users to include any UNIX command inside any simulator input file. The option uses the keyword *SYSTEM* before the UNIX command. This feature authorizes users to include their own simulators or other external routines inside *DeckBuild*. This is what we did to use in *ATHENA*, the new method described above. For example to call a program named 'SCALP' that reads dopant, dose and energy as an input and create as an output a doping profile, we use the syntax illustrated in Figure 5.

```

Deckbuild V3.11.5.R - scalp.in (edited), dir: /home/eric/working_d
File View Edit Find Main Control Commands Tools
go athena
#
line x loc=0.00 spac=0.05
line x loc=0.05 spac=0.05
#
line y loc=0.00 spac=0.0002
line y loc=0.22 spac=0.002
#
nit silicon orientation=100
depo oxide thic=0.01
struc outf=tmp.str
#
-----
set DOP_CAL=Boron
set DOSE_CAL=1e15
set TILT=7
set ROTATION=27
set FITMOD=SCALP
#
-----
# Implantation
system SCALP "$USER"$PID".calib" $DOP_CAL $ENER_CAL $DOSE_CAL
profile $DOP_CAL inf="$USER"$PID".calib"
system rm "$USER"$PID".calib"

set ENER_CAL=1
source IMPLANTATION $DOP_CAL $ENER_CAL $DOSE_CAL $TILT $ROTATION $FITMOD
struc outf=Boron$ENER_CAL$Kev"$DOSE_CAL".str
tonyplot
#
-----
next line stop cont run quit Line: 30
paste init pause clear restart kill Stop: None
ATHENA>
#
ATHENA> #
ATHENA> SYSTEM /home/eric/working_dir/simul/PRODUCT/ATHENA/IMPLANT/SCALP/1D/tishe112
ATHENA> eric.calib Boron 1 1e+15
ATHENA> profile Boron
inf=/home/eric/working_dir/simul/PRODUCT/ATHENA/IMPLANT/SCALP/1D/eric.calib
ATHENA> SYSTEM rm /home/eric/working_dir/simul/PRODUCT/ATHENA/IMPLANT/SCALP/1D/eric.calib
ATHENA> struc outf=Boron1Kev"1e+15".str
ATHENA>
Finished executing line 29 ATHENA

```

Figure 5: Illustration of the 'system' command

The external program 'SCALP' contains the polynomial model that describes the concentration of the dopant as a function of the depth. Figure 6 is an illustration of the profile obtained using SCALP, SVDP and compared to SIMS.

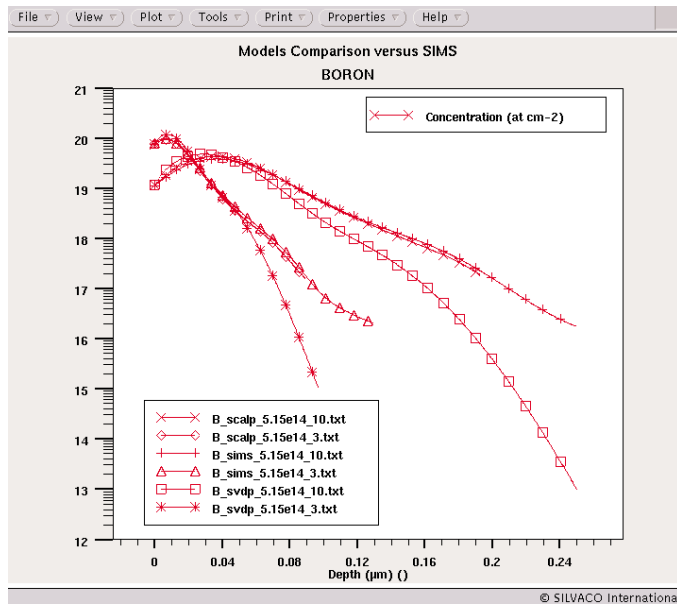


Figure 6: Boron profile resulting from SCALP and SVDP implantation in *ATHENA*

VI. Conclusion

We have developed an efficient technique for predictive simulation of ion implantation. The methodology allows the calibration of As, BF₂ and B profiles, with the knowledge of a confidence interval, for the low energy, high dose conditions of sub-100nm CMOS technology. This new technique can be then applied into *ATHENA*.

References

- [1] Al. F. Tash et al. - J. Elec. Soc. 136(3) 1989 - pp 810-814.
- [2] G. Balamurugan et al. - IEDM'98 - pp 517-520.
- [3] G.E.P. Box, N.R. Draper, John Wiley & sons, N.Y., 1987.
- [4] G. Le Carval et al.- SISPAD'97 - pp 177-180.
- [5] Ph. Holliger et al - Proc. of 13th An. Workshop on SIMS.
- [6] ECHIP 6.4 user's guide.
- [7] SILVACO International - *ATHENA User's Guide*

Using *Luminous* to Model the Transient Response of a Silicon Charge Collection and Transfer Structure

Introduction

The rapid evolution of modern photonic devices in digital photographic and detection systems creates a need for physically-based simulation of charge collection and transfer. In this article we show the linearity, spatial sensitivity, and spectral response of a generalized silicon pixel structure using the *Luminous* module of the *ATLAS* device simulator. The *Luminous* module is used to simulate net charge generation due to incident light energy, and the *S-Pisces* module is used to simulate charge transport and generation-recombination mechanisms using the standard drift-diffusion transport equations coupled with Shockley-Read-Hall, Auger, and optical generation-recombination models.

Pixel Structure

The charge collection structure modeled here is typical of imaging applications, where charge is formed by electron-hole pair generation due to light incident on the silicon substrate. The charge is kept confined laterally by a transfer channel stop, shown in Figure 1 as a thick field oxide outside the active charge transfer region, and a lower concentration

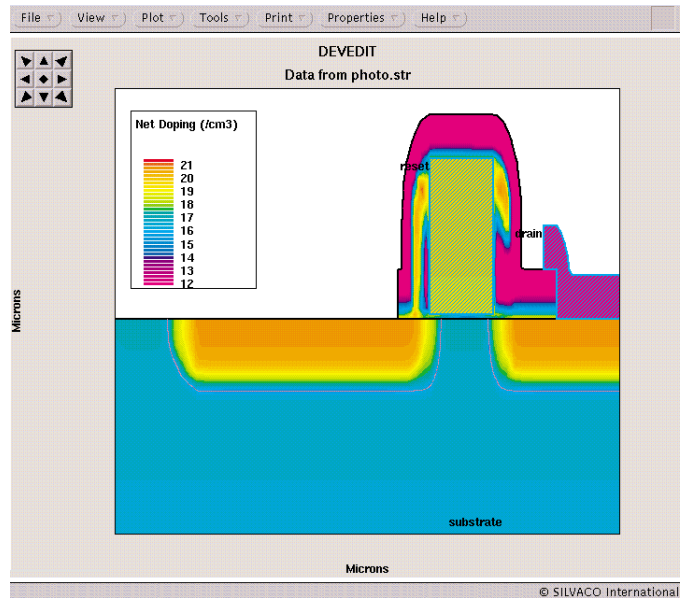


Figure 1. The n-well charge collection and transfer structure.

of phosphorus under the gate region. Generally, the charge transfer in pixel and charge-coupled devices is due to diffusion, drift due to the electric field, and fringing electric field effects. Free charge-transfer is used to simulate these mechanisms by modeling only the free electrons in the conduction band.

Figure 1 shows a generalized phosphorus-doped, polysilicon-gated pixel structure that is used to model linearity, spatial sensitivity, and spectral response of charge collection and transfer mechanisms. The structure was created in the *ATHENA* process module, and the solution grid was then modified for device simulation using the *DevEdit* device editor. The n-well pixel on the left side of the structure is coupled to the n-well drain on the right side by the polysilicon reset gate. The aluminum drain contact is isolated from the reset gate contact by silicon dioxide. As shown in Figure 1, the oxide retains charge from the implant process. Oxide charge is not modeled in this simulation, however, trapped and mobile oxide charge can be simulated using the *ORCHID* module.

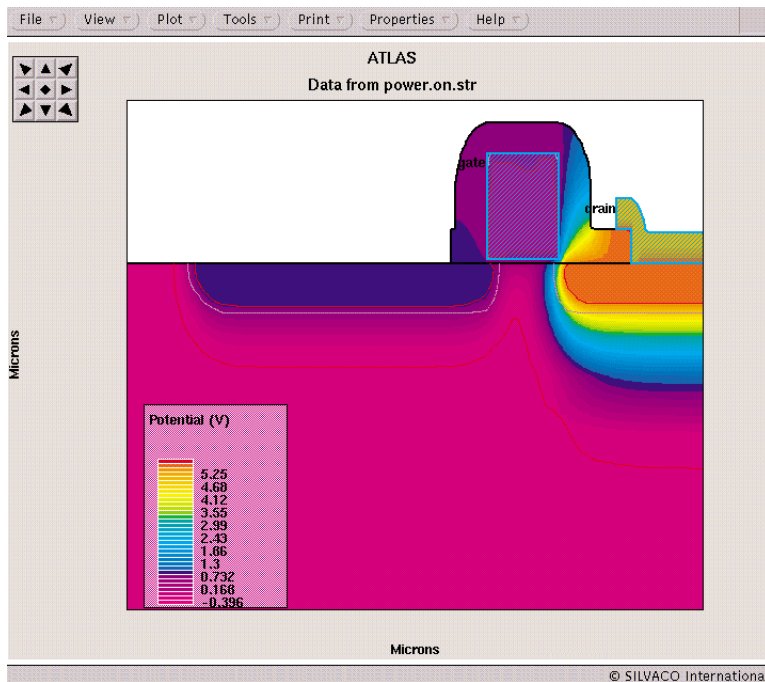


Figure 2. The pixel structure with the drain biased at 5V, showing the metallurgical junction and depletion region edges.

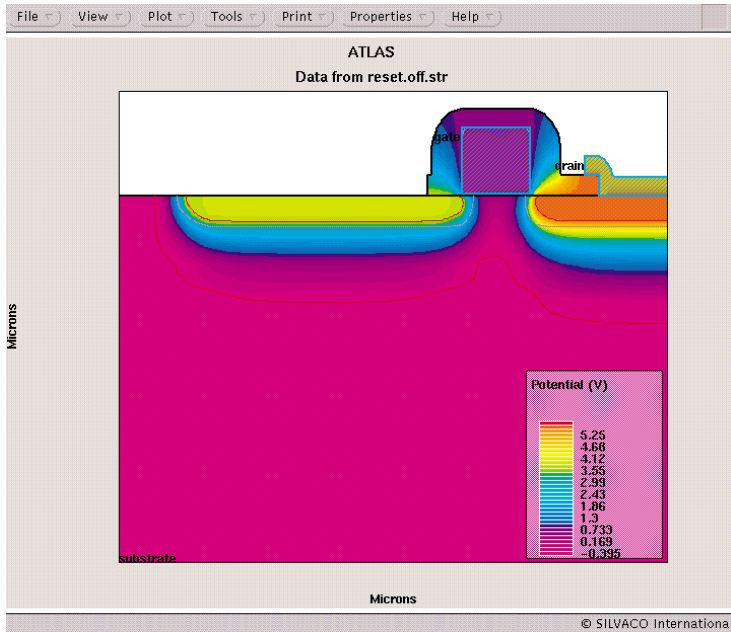


Figure 3. The pixel structure with the reset gate biased at 5V.

To set up the charge collection and transport condition, the drain contact is biased to the 5V steady-state condition with the gate and substrate contacts grounded, as shown in Figure 2. This bias condition drops the drain well potential while keeping the drain isolated from the pixel. The reset gate is then biased to 5V, which lowers the potential under the gate and creates a region of high electron concentration in the n-well, as shown in Figure 3. The gate is then reset to 0V and the structure solution is immediately saved before illumination, as shown in Figure 4.

Transient Simulation Under Illumination

From the setup condition in Figure 4, the transient electrical behavior of the structure is simulated under a sequence of spot powers and frequencies for a duration of 10 ms (ramped from zero to peak intensity over 1ns), to model the linearity, spatial, and spectral response of the pixel. Response curves are extracted from the voltage change just under the surface of the pixel center.

For the transient response of the n-well, consider that as the free electron charge density in the pixel region increases due to irradiated energy, the surface and bulk potential decrease. This change is associated with the filling of the potential well with electrons. For a fixed gate voltage, the surface potential decreases linearly to first order as electron concentration increases. Thus we expect a linear potential and charge collection response in a constant-flux irradiation condition.

Figure 5 shows the linearity of device response with beam intensity at 500nm, corrected for dark current during the transient. Saturation occurs near 60 mW/cm², and the sensitivity of potential and charge is nearly linear at lower intensities, as expected from the discussion above.

Figure 6 shows the spatial response across the entire test structure at 500nm and 10 mW/cm² spot power calculated as the change in potential under the pixel surface center after 10 ms, corrected for leakage current during the transient.

The spectral response of the pixel structure is shown in Figure 7 for wavelengths of 200-1200 nm at 10 mW/cm² spot power during the 10 ms transient, corrected for leakage current. The peak sensitivity occurs near 500 nm, and drops to 50% of the peak sensitivity near 600nm and 350 nm.

It is important to consider the effect of dark current in the characterization of charge transport for this test structure. Dark current is a result of carrier generation in the depletion region, diffusion current at the depletion region edge, and the surface generation current. All these mechanisms are primarily dependent on the minority carrier lifetime, the diffusion constant, the diffusion length, and the surface recombination rate. For the structure considered here, the surface recombination rate is a negligible term compared to lifetimes and diffusion parameters, since the larger area of the pixel storage surface is free of charge coupling

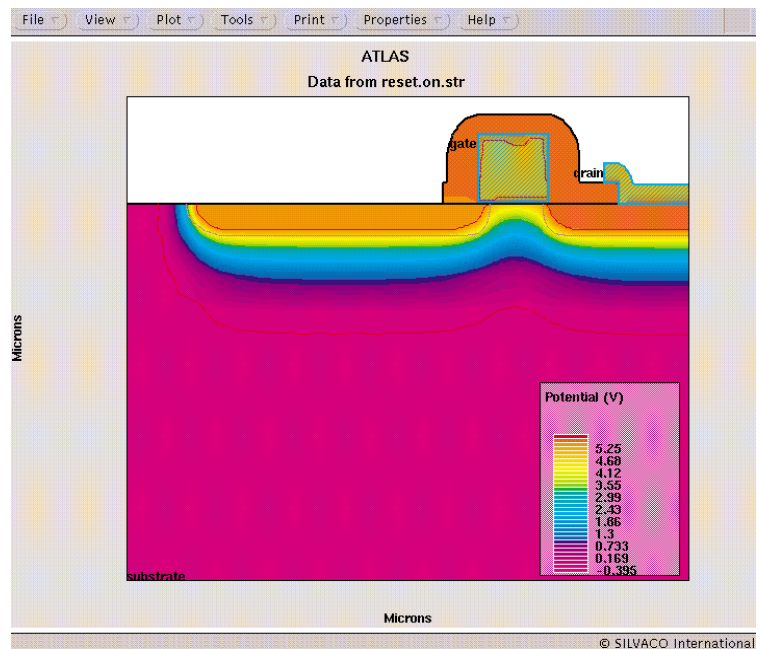


Figure 4. The pixel structure with the gate contact reset to 0V, ready for illumination.

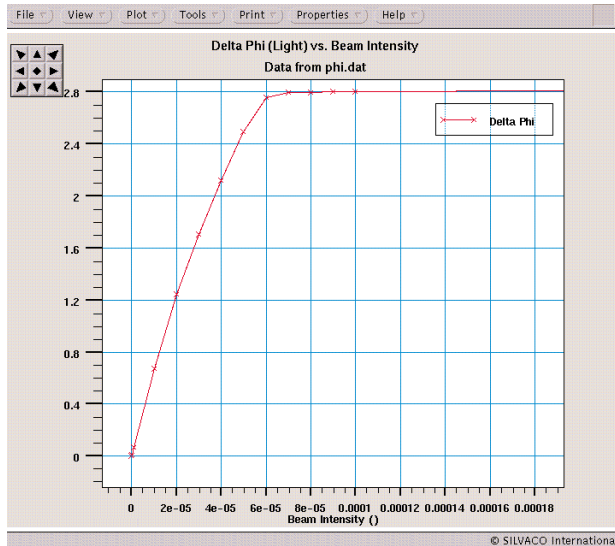


Figure 5. Linearity response of the pixel structure under 500nm illumination for 10 ms.

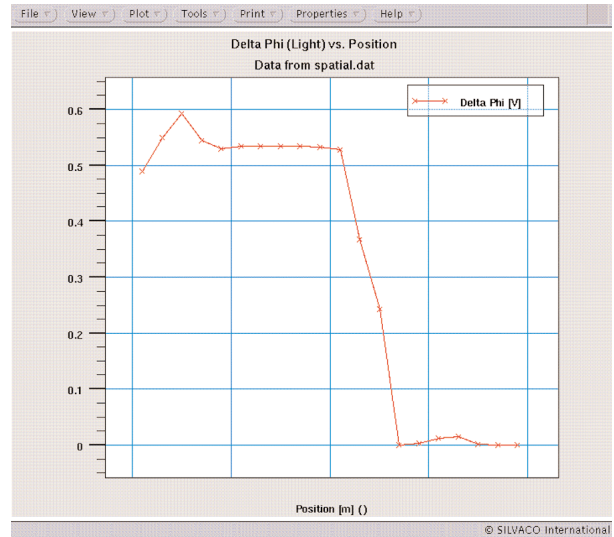


Figure 6. Spatial response across the entire structure under 500nm illumination for 10 ms at 10 mW/cm² spot power.

effects with a surface oxide or electrode which may cause nearly equal electron and hole concentrations, resulting in a large surface recombination rate and surface generation-recombination current. The other components of dark current, depletion region generation and diffusion current, are normalized in this analysis by subtracting the change in potential due to dark current (to first order) by extracting a dark 10 ms transient potential change.

Summary

The step illumination response of a biased pixel structure is modeled using drift diffusion, generation-recombination, and optical models in *ATLAS* and *Luminous*, in the free charge-transfer model, which considers only free electrons in the conduction band. The transition of conduction band electrons to bound states and midgap states, such as interface traps, is typically considered at medium to low frequencies in surface and buried CCDs. Also, trapped and mobile oxide charge under steady-state and transient bias conditions may be optionally modeled in *ORCHID* for devices which exhibit surface effects typically associated with oxide charge.

Spatial sensitivity and spectral response are simulated in the linear range of potential sensitivity to illumination intensity at 10 mW/cm². The peak frequency sensitivity occurs near 500nm, and the n-well charge collection region is the most sensitive part of the structure, as expected. We also note that

charge integration in the n-well pixel (calculations from the *TonyPlot* “Extract” statement, not shown) gives nearly the same results as change in potential, which is the expected result.

References

- [1] S.M. Sze, Physics of Semiconductor Devices, 2nd Ed., John Wiley & Sons, New York, 1981.
- [2] B.G. Streetman, Solid State Electronic Devices, 3rd Ed, Prentice Hall, New Jersey, 1990

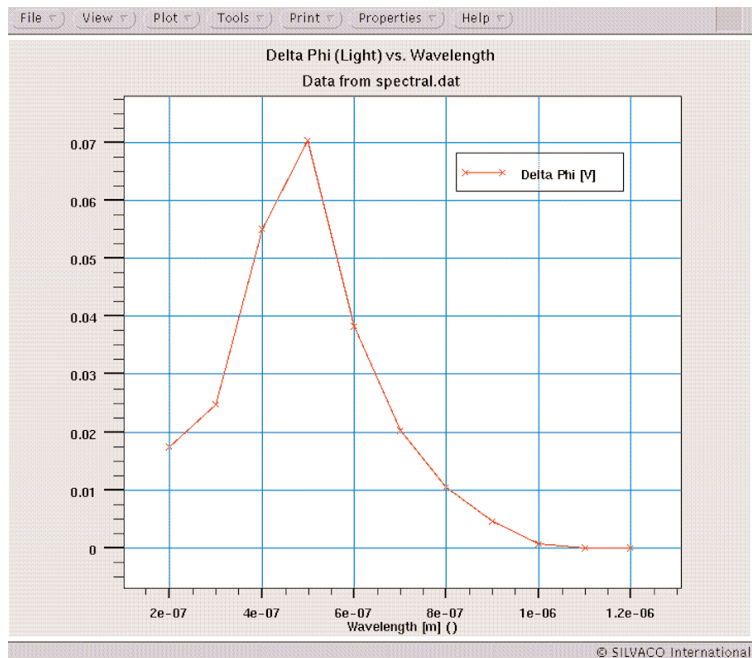


Figure 7. Spectral response of the pixel structure under illumination at 10mW/cm² spot power at 500 nm illumination for 10 ms.

Calendar of Events

May

- 1 GaAs MANTECH -
Washington DC

- 2 GaAs MANTECH -
Washington DC

- 3 GaAs MANTECH -
Washington DC

- 4 GaAs MANTECH -
Washington DC

- 5

- 6

- 7

- 8

- 9

- 10

- 11

- 12

- 13

- 14 IPRM Williamsburg, VA

- 15 IPRM Williamsburg, VA

- 16 IPRM Williamsburg, VA

- 17 IPRM Williamsburg, VA

- 18 IPRM Williamsburg, VA

- 19

- 20

- 21

- 22 ISPSD Toulouse, France
IWCE Glasgow, Scotland

- 23 ISPSD Toulouse, France
IWCE Glasgow, Scotland

- 24 ISPSD Toulouse, France
IWCE Glasgow, Scotland

- 25

- 26

- 27

- 28

- 29

- 30

- 31

June

- 1

- 2

- 3

- 4

- 5 IITC - San Francisco, CA
DAC - Los Angeles, CA

- 6 IITC - San Francisco, CA
DAC - Los Angeles, CA

- 7 IIITC - San Francisco, CA
DAC - Los Angeles, CA

- 8

- 9

- 10

- 11

- 12 HiTEC -Albuquerque, NM

- 13 HiTEC -Albuquerque, NM

- 14 HiTEC -Albuquerque, NM

- 15

- 16

- 17

- 18

- 19

- 20

- 21 EWLTE Noordwijk, -
The Netherlands

- 22 EWLTE Noordwijk, -
The Netherlands

- 23 EWLTE Noordwijk, -
The Netherlands

- 24

- 25

- 26

- 27

- 28

- 29

- 30

Bulletin Board



DAC

Silvaco kicks off the summer with the largest EDA conference of the year. The Design Automation Conference provides us with the opportunity to meet with our valued customers, and provide information about the high quality and outstanding reliability of Silvaco tools.



High Temp. hits Albuquerque

The high desert city of Albuquerque, New Mexico will be hosting The High Temperature Electronics Conference. It begins June 12th and ends on the 15th. This conference re-emphasizes the relationship between Silvaco International and the military's high-tech developers



IWCE

Our simulation software will be showcased this May at the International Workshop on Computational Electronics. Silvaco bolsters its reputation for continued leadership in the EDA industry with tools that define the standards for accuracy and speed.

If you would like more information or to register for one of our workshops, please check our web site at <http://www.silvaco.com>

The Simulation Standard, circulation 18,000 Vol. 11, No. 5, May 2000 is copyrighted by Silvaco International. If you, or someone you know wants a subscription to this free publication, please call (408) 567-1000 (USA), (44) (1483) 401-800 (UK), (81)(45) 341-7220 (Japan), or your nearest Silvaco distributor.

Simulation Standard, TCAD Driven CAD, Virtual Wafer Fab, Analog Alliance, Legacy, ATHENA, ATLAS, MERCURY, VICTORY, VYPER, ANALOG EXPRESS, RESILIENCE, DISCOVERY, CELEBRITY, Manufacturing Tools, Automation Tools, Interactive Tools, TonyPlot, TonyPlot3D, DeckBuild, DevEdit, DevEdit3D, Interpreter, ATHENA Interpreter, ATLAS Interpreter, Circuit Optimizer, MaskViews, PSTATS, SSuprem3, SSuprem4, Elite, Optolith, Flash, Silicides, MC Depo/Etch, MC Implant, S-Pisces, Blaze/Blaze3D, Device3D, TFT2D/3D, Ferro, SiGe, Laser, VCSELS, Quantum2D/3D, Luminous2D/3D, Giga2D/3D, MixedMode2D/3D, FastBlaze, FastLargeSignal, FastMixedMode, FastGiga, FastNoise, Mocasim, Spirt, Beacon, Frontier, Clarity, Zenith, Vision, Radiant, TwinSim, , UTMOST, UTMOST II, UTMOST III, UTMOST IV, PROMOST, SPAYN, UTMOST IV Measure, UTMOST IV Fit, UTMOST IV Spice Modeling, SmartStats, SDDL, SmartSpice, FastSpice, Twister, Blast, MixSim, SmartLib, TestChip, Promost-Rel, RelStats, RelLib, Harm, Ranger, Ranger3D Nomad, QUEST, EXACT, CLEVER, STELLAR, HIPEX-net, HIPEX-r, HIPEX-c, HIPEX-rc, HIPEX-crc, EM, Power, IR, SI, Timing, SN, Clock, Scholar, Expert, Savage, Scout, Dragon, Maverick, Guardian, Envoy, LISA, ExpertViews and SFLM are trademarks of Silvaco International.

Hints, Tips and Solutions

William French, Applications and Support Manager

Q. When I simulate my process flow the simulated profile is always lower than the SRP measurements. What could be causing this ?

In many simulated process flows the surface oxide is etched completely off after which there may be some diffusion cycles. When *ATHENA* performs a diffusion step it will model the diffusion of dopants not only into the silicon but also across region boundaries for instance from silicon to the gas above the silicon surface. So if no oxide is present on the surface of the silicon, dopant loss may occur into the gas. To illustrate a $1e14$ Boron implant @ 50 KeV is performed into silicon and is annealed at 1150C for 60 minutes. Figure 1 shows the resulting Boron profile when an oxide layer is deposited just before the diffusion and when the silicon surface is exposed. Clearly significant dopant may be lost if no oxide is present. It is important therefore to check in each input deck that a surface oxide is present before any diffusion step is performed.

If it is desired to modify this dopant loss the user may adjust the segregation coefficients with the command

```
IMPURITY I.BORON SILICON /GAS SEG.0=1  
SEG.E=0.0 TRN.0=27.9 TRN.E=2.48
```

Q. The structure I am simulating inside *ATHENA* is very large and the number of mesh points has become excessive. Is there anything I can do to get around this limitation ?

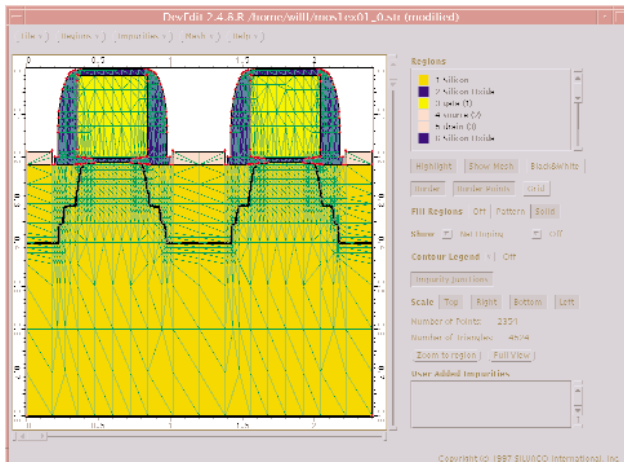


Figure 2: DEVEDIT was used to combine two *ATHENA* structures together to form one single structure which was then remeshed.

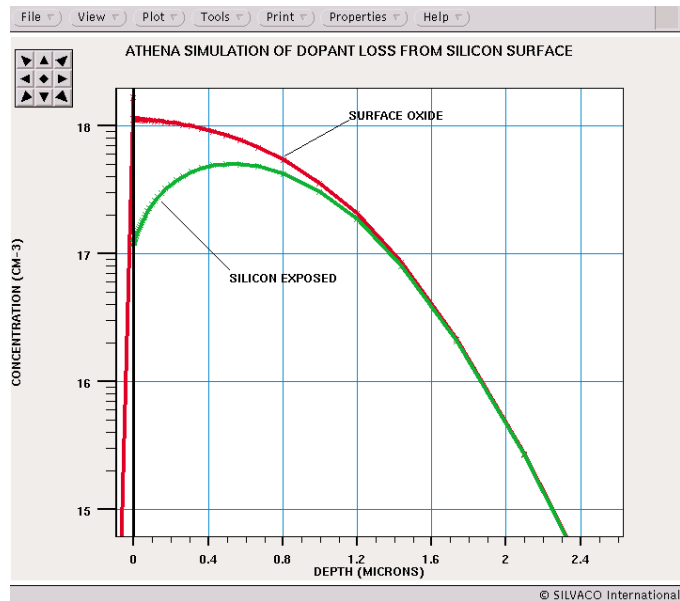


Figure 1. The Boron profile that results when a surface PAD oxide is present compared to the result when it is absent. Significant dopant is lost to the GAS above the silicon surface if no PAD oxide is present.

A possible solution does exist with the application of the Silvaco tool *DevEdit*. This tool allows a user to load one *ATHENA* structure and to then JOIN a second *ATHENA* structure to it. Therefore if the *ATHENA* simulation is very large the *ATHENA* input deck may be broken into two parts. The first may simulate only one half the length of the device whilst the second, which has an identical depth, will simulate the rest. By dividing the simulation domain into two discrete *ATHENA* input decks it is possible to maintain a dense mesh without hitting problems with the number of nodes. To illustrate, the *DeckBuild* example mos1ex01_0.str structure was loaded into *DevEdit* and by use of the "File --> Join" option was then joined to another file (in this case it was also mos1ex01_0.str). When remeshed the final structure is shown in Figure 2.

Call for Questions

If you have hints, tips, solutions or questions to contribute, please contact our Applications and Support Department
Phone: (408) 567-1000 Fax: (408) 496-6080
e-mail: support@silvaco.com

Hints, Tips and Solutions Archive

Check our our Web Page to see more details of this example plus an archive of previous Hints, Tips, and Solutions
www.silvaco.com

Your Investment in Silvaco is SOLID as a Rock!!

While others faltered, Silvaco stood SOLID for 15 years. Silvaco is NOT for sale and will remain fiercely independent. Don't lose sleep, as your investment and partnership with Silvaco will only grow.

SILVACO INTERNATIONAL

USA HEADQUARTERS

Silvaco International
4701 Patrick Henry Drive
Building 2
Santa Clara, CA 95054
USA

Phone: 408-567-1000
Fax: 408-496-6080

sales@silvaco.com
www.silvaco.com

CONTACTS:

Silvaco Japan
jpsales@silvaco.com

Silvaco Korea
krsales@silvaco.com

Silvaco Taiwan
twsales@silvaco.com

Silvaco Singapore
sgsales@silvaco.com

Silvaco UK
uksales@silvaco.com

Silvaco France
frsales@silvaco.com

Silvaco Germany
desales@silvaco.com

*Products Licensed through Silvaco or e*ECAD*

